

## Technical Note

# Numerical analysis and monitoring of a rockfill dam at the end of construction (case study: Vanyar dam)

M. Derakhshandi<sup>1\*</sup>, H. R. Pourbagherian<sup>2</sup>, M. H. Baziar<sup>3</sup>, N. Shariatmadari<sup>4</sup>, A. H. Sadeghpour<sup>5</sup>

Received: December 2013, Revised: April 2014, Accepted: June 2014

## Abstract

*In this study, the mechanical behavior of Vanyar dam was evaluated at the end of construction. A two-dimensional numerical analysis was conducted based on a finite element method on the largest cross-section of the dam. The data recorded by the instruments located in the largest cross-section were compared with the results of the numerical analysis at the place of instruments. The settlement, pore water pressure, and total vertical stress were the parameters used for evaluating the dam behavior at the end of construction. The results showed that the settlements obtained from the numerical analysis were in reasonable agreement with the data recorded by the instruments, which proved that the numerical analysis was implemented based on realistic material properties. In addition, the difference between the instruments and the numerical analysis in terms of total vertical stresses was discussed by focusing on the local arching around the pressure cells. Furthermore, the arching ratios were calculated based on the results of the numerical analysis and the data recorded by the instruments. Moreover, the pore water pressures and total vertical stresses, recorded by piezometers and pressure cells, respectively, were the two parameters utilized for evaluating the hydraulic fracturing phenomena in the core. The results demonstrated that the maximum settlement obtained from the numerical analysis was 1 m, which corresponded to 46 m above the bedrock on the core axis. The recorded data in the core axis indicated that maximum settlement of 0.83 m happened 40 m above the bedrock. In addition, maximum pore water pressure ratio recorded by the instruments ( $R_u = 0.43$ ) was more than that obtained from the numerical analysis ( $R_u = 0.26$ ); this difference was due to the local arching around the pressure cells. Furthermore, the arching ratios in Vanyar dam were found to be 0.83 to 0.90. In general, the results revealed that the dam was located on a safe side in terms of critical parameters, including settlement and hydraulic fracturing. In addition, results of the numerical analysis were consistent with those provided by the monitoring system.*

**Keywords:** Rockfill dam, 2D-numerical analysis, Monitoring, Back analysis, Vanyar.

## 1. Introduction

Behavior of earth dams during construction and operation is a crucial issue in terms of settlement and hydraulic fracturing, which may cause serious hazards to dams and their associated facilities. Because of some uncertainties in material properties, results of a numerical analysis may be somehow different from those provided by instruments. Hence, back analysis of dams is necessary at the end of construction.

By designing a monitoring system and installing the corresponding instruments in the body of a dam during construction, settlements, stresses, and pore water pressures can be measured. Analysis of the data recorded by the instruments not only helps to understand the complicated stresses and settlements in the body of the dam, but also can be a suitable basis for determining the geotechnical parameters through the back analysis. These data can be compared with the numerical results to assess the accuracy of numerical analysis. According to the earth dam codes, the results of a numerical analysis are acceptable provided that there is a tolerable difference between these results and those provided by the instruments. If the difference is significant, it will then be necessary to perform a kind of back analysis to modify the material properties and assumptions [1].

Clough and Woodward [2] carried out some stress-strain analyses on a homogeneous embankment over rigid subsoils, the results of which showed that, to correctly simulate the construction process, it is necessary to consider incremental

\* Corresponding author: m.derakhshandi@gmail.com

1 Assistant professor, Department of Civil Engineering, Science and Research Branch, Islamic Azad University, Tehran, Iran

2 M.Sc. Faculty of Engineering, Arak University, Arak, Iran

3 Professor, Department of Civil Engineering, Iran University of Science and Technology, Tehran Iran

4 Professor, Department of Civil Engineering, Iran University of Science and Technology, Tehran Iran

5 Assistant Professor, University of Kashan

stage construction in comparison to single stage construction. In addition, the vertical stresses obtained from both analyses had nearly the same values, while the difference of settlement was significant. Nailure et al. [3] conducted back analysis on the largest cross-section of the Beliche dam in the southwest of Portugal. In this analysis, the settlements obtained from a two-dimensional numerical analysis were compared with those recorded by instruments at the end of construction. The results revealed that the settlements and total vertical stresses recorded by the instruments were in good agreement with those obtained by the numerical analysis at the axis of the dam. Furthermore, they concluded that the difference of settlements was related to the variation of the material characteristics between the laboratory and material resources and the creep. Additionally, the difference of total vertical stresses was due to some problems in stress measurement by pressure cells. Arching ratio is an important parameter which can evaluate the hydraulic fracturing at the end of construction. Hunter [4] studied the effect of core width on arching ratio during construction and the results showed that arching ratio for wide cores was considerably less than the one for the narrow cores of earth dams. In addition, total vertical stresses at the center of a core increased by an increase in the width of the core. Yuzhen et al. [1] carried out back analysis on the Maopingxi rockfill dam in China and showed that genetic algorithms and artificial neural networks can be used as powerful tools beside numerical analyses to perform back analysis of earth dams. Back analysis of Mornos dam was another study which was undertaken by Gikas and Sakellariou. [5] and aimed to study the behavior of Mornos dam during 30 years after its construction in terms of settlements. In this study, the settlement data recorded by continuous geodetic monitoring were compared with those obtained from the numerical analysis. The results revealed that the settlements recorded by the geodetic monitoring system and the numerical analysis were in good agreement; thus, the procedure can be used for monitoring the lifetime of earth dams.

Settlement behavior of Shuibuya CFRD dam during construction, initial filling of reservoir, and two years after operation was assessed by Zhou et al. [6]. They carried out two-dimensional numerical analysis using FEM and compared the results with the data measured by the instruments in terms of settlements. In addition, back analysis was performed by utilizing hybrid generic algorithms (HGAs). The results represented this technique as a successful one for controlling the dam deformation. Furthermore, the results demonstrated that settlement increased apparently after the initial filling of reservoir; but, rate of settlement decreased and tended to stabilize over time.

Mahin Roosta and Alizadeh [7] assessed the nonlinear behavior of rockfill material through numerical analysis and laboratory tests. To estimate of the collapse settlement phenomena in the rockfill dam during inundation, strain hardening and strain softening model in Flac software were modified based on the data provided from the laboratory test. The results helped dam engineers to have better prediction of nonlinear behavior and collapse settlements in the upstream shell.

Weixin et al. [8] simulated the numerical behavior of

Nuozhadu rockfill dam constructed on Lancang River. Two constitutional models including Duncan and Chang's EB model and the modified generalized plasticity model proposed by Pastor, Zienkiewicz, and Chan (PZ-III) were used in the same FEM framework to evaluate the stress-strain behavior of this dam after the initial filling of its reservoir. Then, in-situ monitoring data were compared with the corresponding results of the numerical analyses and results showed that the modified PZ-III model can predict better description of deformation in comparison to Duncan and Chang's EB model. In addition, the modified PZ-III can evaluate the coarse material data including nonlinearity, dilatancy, and pressure dependency.

Ghanbari and Shams Rad [9] evaluated hydraulic fracturing in the core of the earth dams through the laboratory tests and numerical analysis of Vanyar Dam. Advanced Rowe cell was applied for laboratory tests which was performed on unsaturated specimens in unconsolidated conditions. Three types of soils, including CL, SC, and GM-GC, were used in laboratory tests and results revealed that, for fine-grained soils and coarse-grained soils containing considerably fine percent of particles, initial hydraulic fracturing pressure was a linear function of minor principal stress and increased by increasing stress. In addition, the results of numerical analysis on the largest cross-section of Vanyar dam depicted that CL was susceptible to hydraulic fracturing and use of GM-GC was recommended.

Vanyar dam is a rockfill dam constructed near city of Tabriz, Iran. Tabriz is located in a very tectonized region with a high potential for seismicity. Providing a supply of salt-free fresh water has been the major aim of constructing this dam. There are a few river branches in this catchment basin, including fresh and salt water. Some evaporating dams have been constructed across salt-water rivers in order to prevent them from flowing to the reservoir of Vanyar dam.

In this study, the mechanical behavior of Vanyar dam was evaluated at the end of construction using Geo-studio software [10], which is based on finite element method (FEM). The numerical analysis was conducted based on the plane strain modeling of the largest cross-section of the dam. Settlement, pore water pressure, and vertical total stress were the crucial parameters which were extracted from the numerical analysis and compared with those recorded by the instruments at the end of the dam construction. On the basis of the data recorded through the monitoring system, validation of the assumed material properties was confirmed in the numerical analysis. In addition, susceptibility of the hydraulic fracturing was assessed by calculating the arching ratio.

## 2. Main Features of Vanyar Dam

Vanyar dam is a part of Ajichai project, located 5 km to the north east of city of Tabriz, Iran and has been constructed on Ajichai River. Main objectives of the dam construction include agricultural water supply, salinity removal of Ajichai water, and flood control. Height of the dam from the bedrock and the riverbed is 91m and 39 m, respectively, in the largest cross-section. Length of the crest is also about 278 m.

There is depth of about 52 m from the excavation point at

the riverbed down to the bedrock. Two layers of filters on upstream and downstream support the vertical clay core and the transient shell located between the clay core and rockfill shell. In addition, the upstream face is supported by riprap. Fig. 1 shows different zones of cross-section C (the largest cross-section of the dam) as well as layout of the inclinometers, settlement measuring devices, pressure cells, and piezometers.

and piezometers at five levels of the height in the dam. The dam construction started in 2002 and ended in 2011. Its instrumentation started in 2003 and the data were continuously recorded during the construction. Most of the instruments were concentrated in the clay core. Table 1 shows the main technical characteristics of the dam and its reservoir.

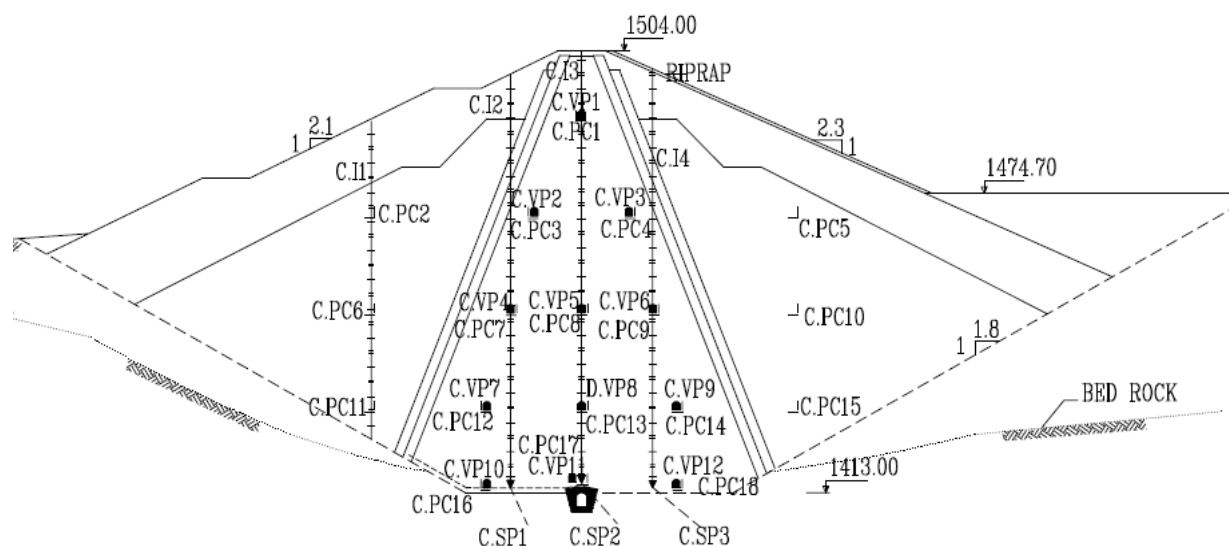


Fig. 1 The layout of the settlement tubes, inclinometers, pressure cells, and piezometers in cross-section C [15].

Table 1 Technical characteristic of the Vanyar dam and its reservoir [15]

| Dam detail   | Value                          |
|--|--------------------------------|
| Height of crest from bedrock (in the largest cross-section)    | 91m                            |
| Height of crest from river bed ((in the largest cross-section) | 39m                            |
| Dam crest elevation a.s.l                                      | 1504m                          |
| Normal water level a.s.l                                       | 1498m                          |
| Length of dam crest  | 278m                           |
| Width of dam crest   | 10m                            |
| Total dam volume   | $3.61 \times 10^8 \text{ m}^3$ |
| Dam body materials volume                                      | $1.7 \times 10^6 \text{ m}^3$  |
| Dam slope up-stream  | 1:2.3                          |
| Dam slope down-stream  | 1:2.1 + Berm                   |
| Total reservoir area   | 12.33 Km <sup>2</sup>          |

### 3. Material Properties and Numerical Modeling

Vanyar dam was modeled using Geo-studio software [10], which works based on FE method. Stage construction of soil layers, boundary conditions in geotechnical construction, and excavation projects were applied through the activation or deactivation of the soil elements in an FE model. In addition, a hyperbolic constitutive model (Duncan and change [11]) was used to simulate the

mechanical behavior of the soil in the body of the dam, while elastic perfectly plastic model was applied to the rock, alluvial foundation, and disposal materials as constitutive models in the simulation.

#### 3.1. Material properties

The material properties used in the numerical analysis were extracted from certain soil mechanical laboratory tests on the fine and coarse materials of the dam. Table 2 shows the parameters of hyperbolic constitutive model for various zones of the dam.

As reported in the table,  $\phi$ ,  $C$ ,  $R_f$ ,  $k_b$ ,  $k_{ur}$ ,  $k_l$ ,  $m$ ,  $n$ , and  $n$  are, respectively, hyperbolic constitutive parameters including friction angle, cohesion, failure ratio, bulk modulus number, loading-unloading modulus number, loading modulus number, bulk modulus exponent, modulus exponent, and porosity, respectively. Furthermore, the elastic perfectly plastic model incorporating a Mohr-Coulomb failure criterion as a yield surface was used to simulate the mechanical behavior of the foundation, alluvial, and disposal materials. The parameters of elastic perfectly plastic model for simulating the alluvial foundation, bedrock, and disposal materials which were extracted from the laboratory and field tests are shown in Table 3.

**Table 2** List of the material properties in the numerical analysis [15]

| Material type   | Material properties |        |       |     |     |          |       |       |                                     |                                      |                    |      |
|-----------------|---------------------|--------|-------|-----|-----|----------|-------|-------|-------------------------------------|--------------------------------------|--------------------|------|
|                 | $\phi$ (deg)        | C(kPa) | $R_f$ | m   | n   | $k_{ur}$ | $k_b$ | $k_l$ | $\gamma_{dry}$ (kN/m <sup>3</sup> ) | $\gamma_{bulk}$ (kN/m <sup>3</sup> ) | k(m/s)             | n    |
| Filter          | 33                  | 0      | 0.7   | 0.5 | 0.6 | 600      | 300   | 300   | 18.5                                | 19.5                                 | 10 <sup>-5</sup>   | 0.45 |
| Transient shell | 38                  | 0      | 0.7   | 0.3 | 0.4 | 1200     | 550   | 600   | 20.27                               | 21.27                                | 10 <sup>-4</sup>   | 0.25 |
| Rockfill shell  | 48                  | 0      | 0.9   | 0.5 | 0.7 | 1350     | 800   | 650   | 19.25                               | 19.75                                | 10 <sup>-4</sup>   | 0.25 |
| Clay core (CU)  | 21                  | 15     | 0.72  | 0.4 | 0.5 | 500      | 220   | 250   | 20.04                               | 20.74                                | 5×10 <sup>-8</sup> | 0.35 |

**Table 3** List of the material properties of foundation (Elastic perfect plastic model) [15]

| Material type       | Material properties |       |                       |              |        |  |  |                  |      |
|---------------------|---------------------|-------|-----------------------|--------------|--------|--|--|------------------|------|
|                     | E(kPa)              | $\nu$ | C(kN/m <sup>2</sup> ) | $\phi$ (deg) | $\psi$ | $\gamma_{\text{sat}}$ (kN/m <sup>3</sup> ) | $\gamma_{\text{dry}}$ (kN/m <sup>3</sup> ) | k(m/s)           | n    |
| Alluvial foundation | 35000               | 0.3   | 20                    | 30           | 2      | 20.51                                      | 19.23                                      | 10 <sup>-4</sup> | 0.30 |
| Bedrock             | 390000              | 0.37  | 60                    | 50           | 8      | 21   | 20   | 10 <sup>-9</sup> | 0.25 |
| Disposal            | 30000               | 0.35  | 0                     | 28           | 0      | 19.6                                       | 19.2                                       | 10 <sup>-5</sup> | 0.30 |

In this table, E,  $\nu$ , C,  $\phi$ , and  $\psi$  correspond to Mohr-Coulomb criteria including elastic modulus, Poisson ratio, cohesion, friction angle, and dilation angle, respectively.

To determine the pore water pressure in the dam under the riverbed level, a time-dependent analysis was required to be performed. Volume water content ( $\theta_w$ ) is a parameter, which refers to the correlation between pore water pressure and volume of water in the soil pores [12]. Equation 1 shows the relationship between  $\theta_w$ , saturation ratio (S), and porosity (n) [10].

$$\theta_w = n \cdot S \quad (1)$$

There are some advanced laboratory facilities to predict  $\theta_w$ . In addition, there are some mathematical functions based on numerical methods, which can predict  $\theta_w$  as a function of permeability, particle-size distribution, and soil porosity. In this research,  $\theta_w$  was determined based on the aforementioned functions that were used to do the numerical analysis of Vanyar dam.

### 3.2. Numerical modeling and analysis

The settlements, stresses, and pore water pressures were the important parameters extracted from the numerical analysis at the end of the dam construction. The numerical analysis was conducted based on the FEM on a plane strain model of Vanyar dam. In addition, the numerical simulation included three stages.

First, to calculate the in-situ stresses, the riverbed had to be modeled before the dam construction. In this stage, the horizontal stresses were estimated by applying at rest lateral pressure factor [13].

Second, it was needed to model the cut-off trench excavation to reach the bedrock before starting the dam construction. The cut-off trench excavation was simulated in 12 layers in the software.

Third, the construction of the dam from the bedrock up to the dam crest included two phases:

1. Construction of the dam from the bedrock (1413 m a.s.l) to the riverbed level (1477 m a.s.l), which was simulated in 14 layers with the thickness of 4.55 m in the software and physically took about 6 years. The ground water table at the site of the dam was about the riverbed level. When the height of the dam reached 37 m above the bedrock, underground water was allowed to seep into the body of the dam. Core of the dam was assumed consolidated undrained (CU), because it took a long period to construct the dam in this stage. Due to the low permeability of the clay core, the clay material was gradually saturated, while the level of water in the shell and the alluvial foundation remained constant because of higher permeability of these materials than the clay core. After the saturation of the clay core and when the level of the back filling approximately reached the riverbed level, a steady state of seepage appeared.

2. Construction of the dam from the riverbed level to the dam crest (1504 m a.s.l), which was simulated in six layers. In this phase, the construction operation took about 2.5 years and the clay core was assumed consolidated undrained (CU). All the piezometers started recording the pore pressure in the core of the dam when the water level reached 39 m above the bedrock for the first time (May 21, 2005). It was the time to commence data recording and perform the time-dependent analysis.

At the beginning of the second phase, the water level reached a steady state in the core. Therefore, the excessive pore pressure can be estimated using Equation 2 [14]:

$$\Delta u = B\Delta\sigma_3 + AB(\Delta\sigma_1 - \Delta\sigma_3) = \Delta u_b + \Delta u_a \quad (2)$$

where A and B are Skempton coefficients.

Fig. 2 shows the finite element model of cross-section C. Four-node quadrilateral elements with a maximum length-to-width ratio of 2 were used for meshing. In addition, three-node triangular elements were used in some parts of the dam.

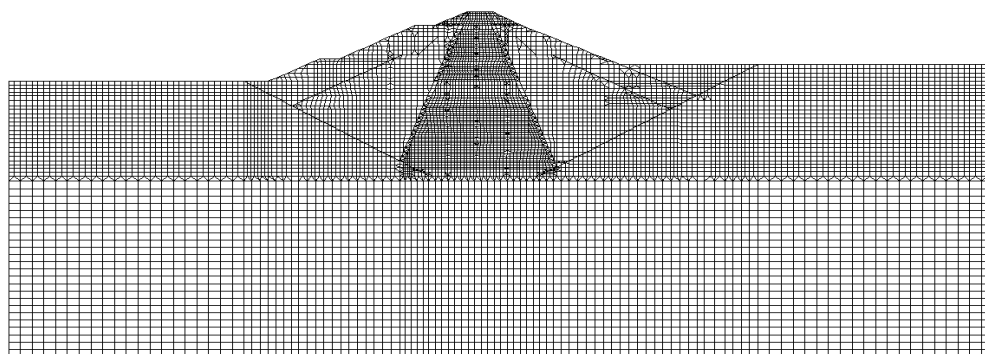


**Fig. 2** Mesh generation of the body and foundation of the dam at cross-section C

## 4. Results and Discussion

In this section, results of the numerical analysis of Vanyar dam including settlements, total vertical stresses, pore water pressures, and arching ratio are compared to the recorded data obtained by the instruments. The results are discussed in the upcoming section.

### 4.1. Settlement results

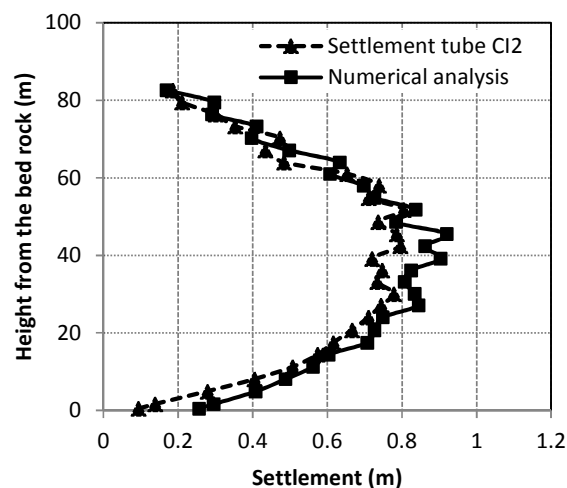
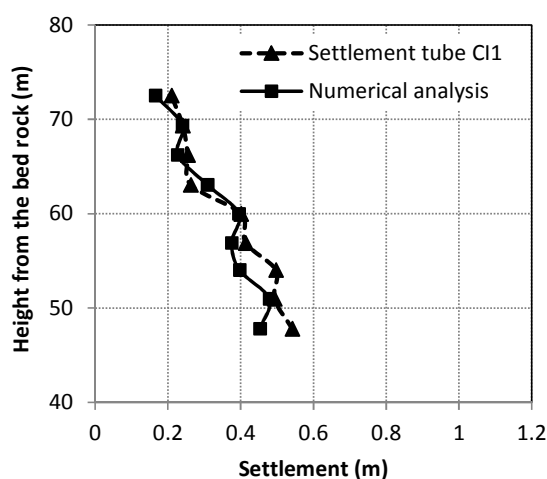
The internal settlements of the dam are categorized into three groups: vertical, horizontal, and rotational movements. Vertical movements show the settlements in terms of material weight, compaction, and consolidation of the dam body. Horizontal movements mainly refer to the upstream movements that occur during impounding in the dam storage, which is due to faster reduction of the effective stress in the upstream materials than in other parts of the dam. Downstream movement is due to the horizontal water pressure of the dam storage. Furthermore,

rotational movements that appear in the upstream and downstream slopes are because of lower shear strength of materials in the foundation or body of the dam. Using surveying points, inclinometers (settlement tubes), and/or settlement gauges is a conventional way for measuring these deformations in earth dams. In this study, an evaluation was made of the results of the vertical deformations in the cross-section C of Vanyar dam obtained from the settlement tubes including CI1, CI2, CI3, and CI4 (Fig. 1).

CI2, CI3, and CI4 were installed from the bedrock to the external surface of the dam in the core. Table 4 shows the maximum vertical settlements obtained from the numerical analysis and use of instruments. Variation of vertical settlements obtained from the numerical analysis and the data recorded by the CI1, CI2, CI3, and CI4 instrument tubes in cross-section C are respectively illustrated in Figs. 3.a, 3.b, 3.c, and 3.d. Results of the vertical settlements showed a good correspondence between the numerical analysis and the data recorded by the instrument in cross-section C.

**Table 4** Maximum vertical settlement for the numerical analysis and instruments

| Instruments No. | Location and distance to dam axis | Maximum settlement (m) |                    | Maximum level of settlement a.s.l (m) |                    |
|-----------------|-----------------------------------|------------------------|--------------------|---------------------------------------|--------------------|
|                 |                                   | Instrument             | Numerical analysis | Instrument                            | Numerical analysis |
| CI1             | D/S (44.4)                        | 0.542                  | 0.479              | 1460.8                                | 1464               |
| CI2             | D/S (15)                          | 0.805                  | 0.92               | 1464.8                                | 1458.5             |
| CI3             | DAM AXIS (0)                      | 0.846                  | 1.06               | 1453.1                                | 1459.2             |
| CI4             | U/S (15)                          | 0.828                  | 0.91               | 1467.5                                | 1458.1             |



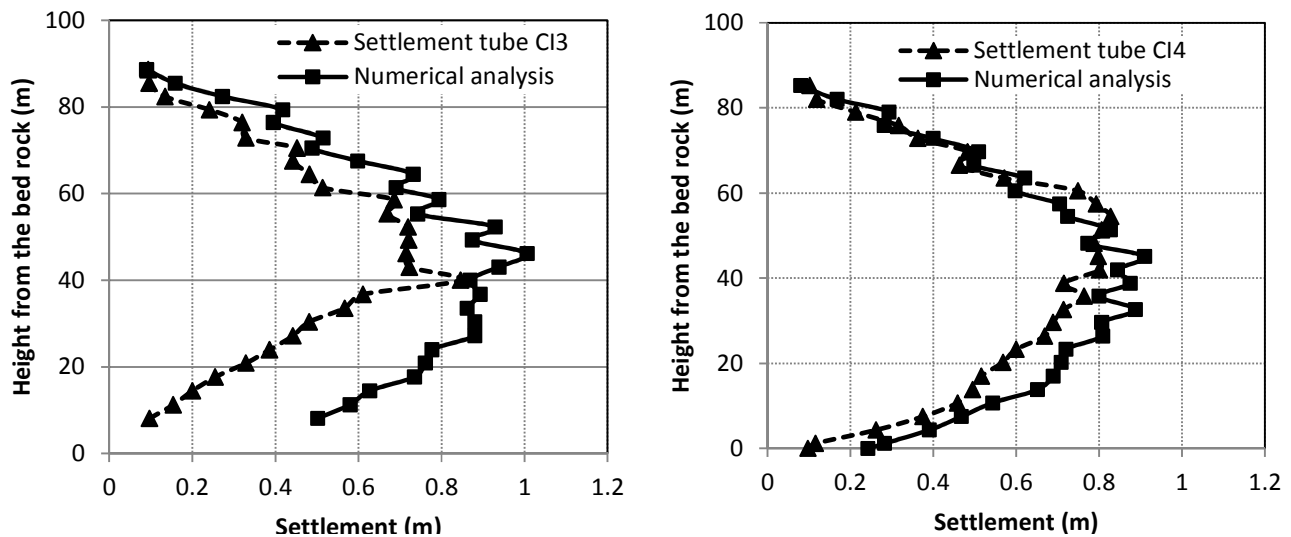


Fig. 3 Comparison of settlements of instruments CI1, CI2, CI3, and CI4 and the numerical analysis of cross-section C

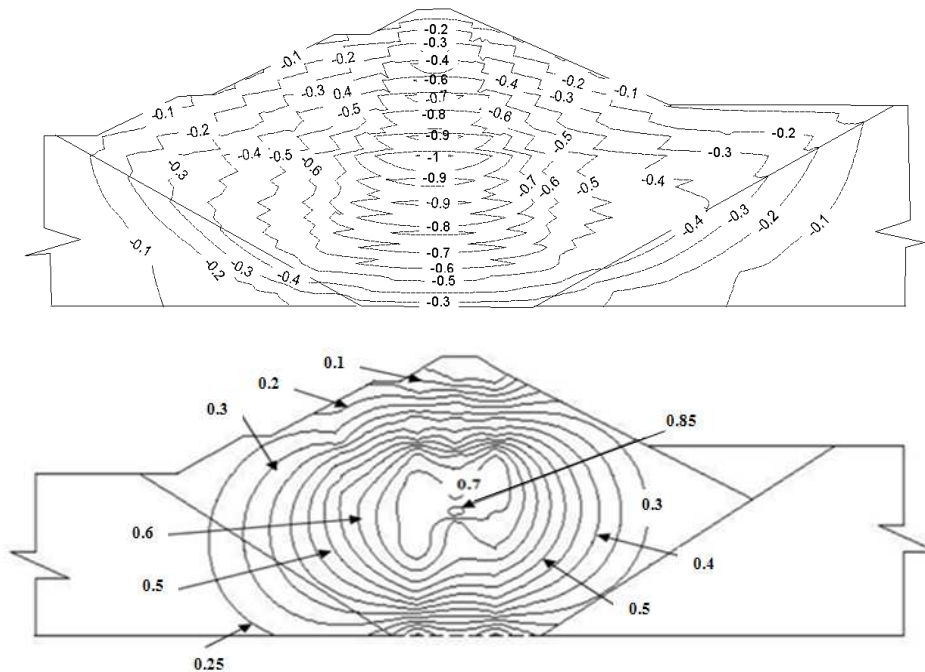


Fig 4 Comparison of settlement contours at the end of dam construction for a. numerical model and b. instruments

The data recorded in settlement tubs, placed in a suitable situation in the body of the dam, were compared with the results of numerical analysis in the place of these settlement gauges at the end of the dam construction through drawing settlement contours, as given in Fig.4. Comparing the contours of settlements in the figure showed good agreement between the recorded settlements and the numerical results. The asymmetry in the contours of instruments was due to the lack of instruments in some parts of the dam body.

As reported in Figs. 3a, 3b, 3c, and 3d, there were some differences between the data recorded by the magnetic settlement tubes and those obtained from the numerical analysis. Maximum settlement, measured at settlement tube CI3 in the axis of the core, was nearly compatible with the numerical analysis. Maximum settlement was recorded about 40 m above the bedrock (

$\frac{z}{h} = 0.44$ ) which was about 0.85 m. In addition, as demonstrated by the numerical analysis, there was the settlement of about 1 m which was located 46 m above the bedrock ( $\frac{z}{h} = 0.51$ ) in the core axis. Maximum settlements corresponding to tube CI1, located in the down-stream shell, were recorded as about 0.54 m (Fig. 3.a), indicating good agreement with the numerical analysis.

There was a significant difference in settlements between the instrument data and the numerical analysis due to the initial delay in supplying and installing the settlement tubes, which can be observed in tube CI3 (Fig. 3.c) [15]. These instruments were installed in the dam axis after back filling by drilling in the constructed backfill. Therefore, there were no recordings by the instruments within this limited time and the observed differences were probably due to this problem.

#### 4.2. Vertical stress and arching ratio

Shell materials including rockfill and gravel were stiffer than the materials used in the core. Difference of elasticity modulus between these two kinds of materials made various tendencies to settlement. In addition, the friction between the core and shell materials caused a transfer of stress from the core to the shell, which could create a low-stress area in the core; this phenomenon is called Arching in earth dams. Equation 3 presents the arching ratio:

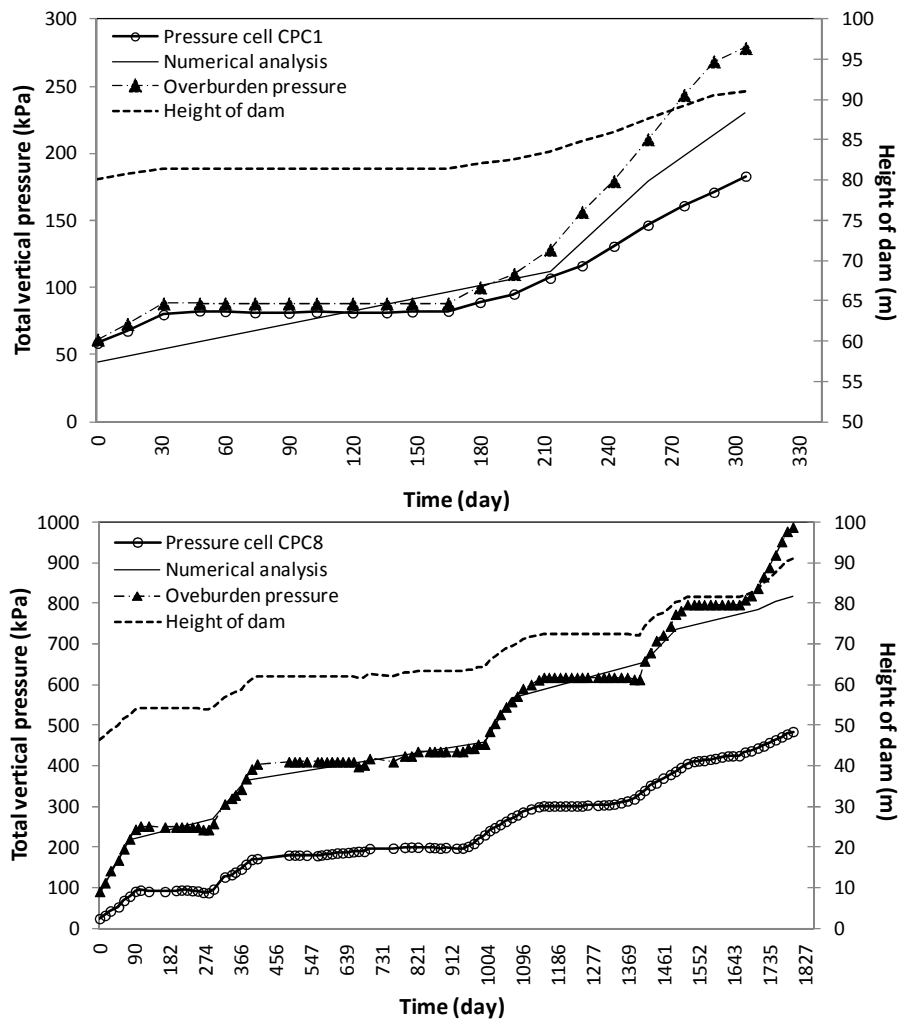
$$A_r = \frac{\sigma_v}{\gamma h} \quad (3)$$

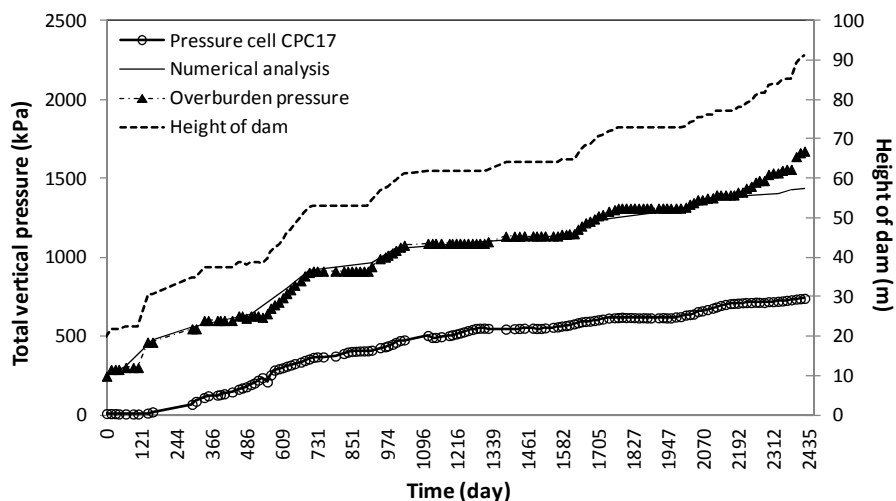
where  $\sigma_v$ : is vertical total stress and  $\gamma h$ : is soil overburden pressure at the point [16, 17].

Vertical stress is a major factor to prevent the creation of cracking in the core. During construction and first impounding, decreased vertical stress due to arching phenomenon can make horizontal cracks, because water

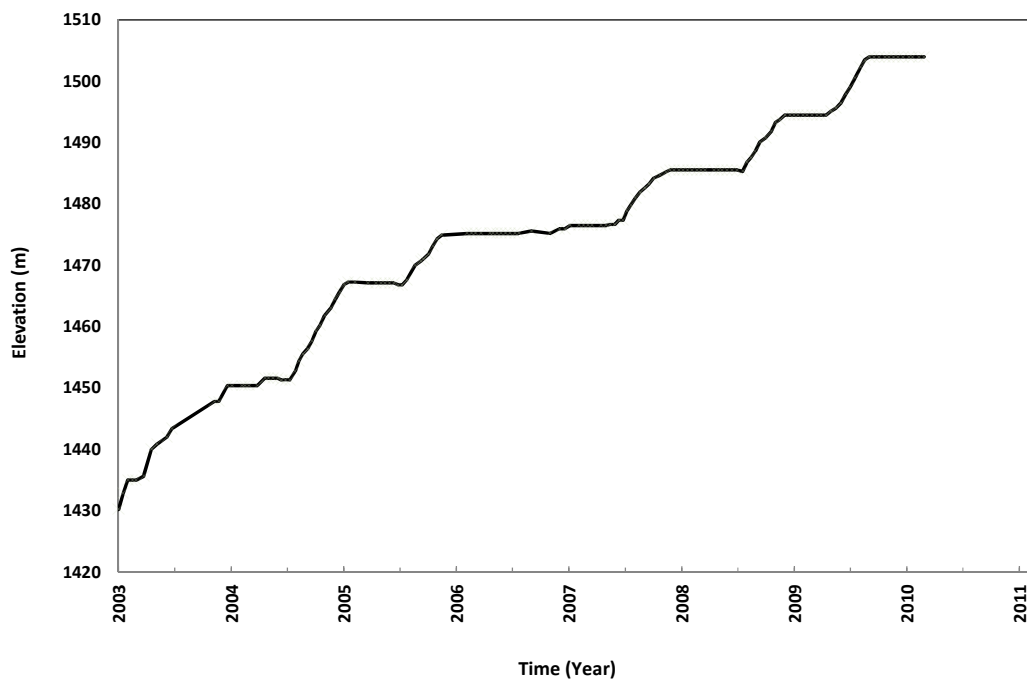
pressure is higher than vertical stress. These cracks are called hydraulic fracturing that makes holes from upstream to downstream. Also, it makes a serious damage to the body of the dam, possibly leading to the dam failure. To prevent arching in the core, arching ratio should be less than 1 in the location of the pressure cells in the core. The higher the  $A_r$ , the less the arching phenomenon in the core and the lower the probability of hydraulic fracturing would be.

The vertical stresses recorded by the pressure cells and results of the numerical analysis during the construction are compared in Fig. 5 for CPC1, CPC 8, and CPC 17 in the core. Each chart contains four curves, including the vertical stresses recorded by the pressure cells and the numerical analysis, and the overburden pressure. Furthermore, variation in the elevation of the dam during construction versus time is shown in Fig.6. To assess the vertical stresses in the depth of the dam, the results of the instruments and numerical analysis are compared in Figs. 7.a, 7.b, and 7.c for the up-stream, center, and down-stream of the core, respectively. In addition, the vertical stresses and arching ratio are compared in Table 5.

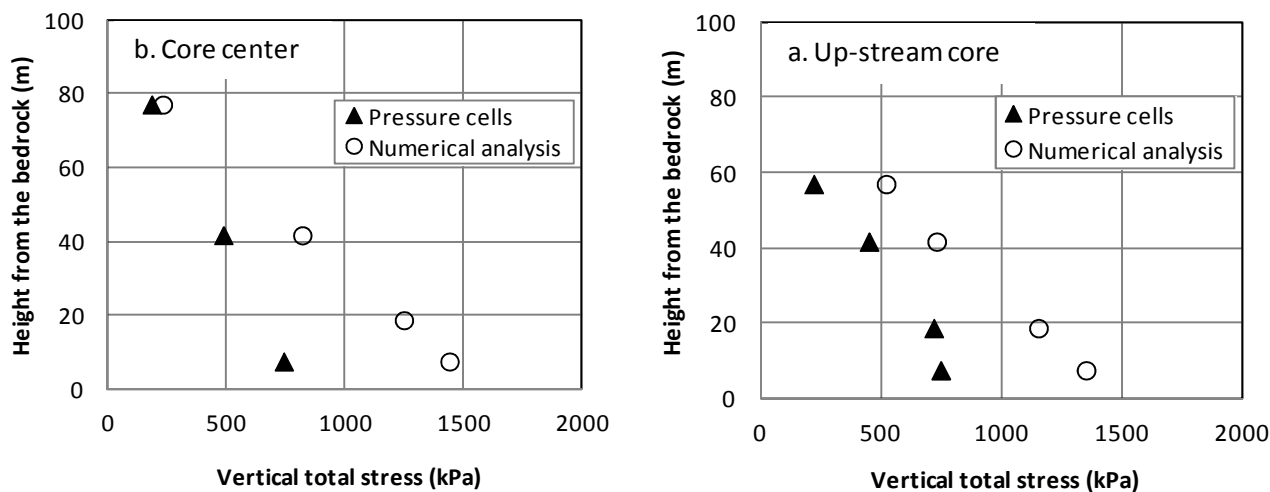




**Fig. 5** Comparison of the recorded data from pressure cells CPC1, CPC8, and CPC17 with those obtained by the numerical analysis during construction



**Fig. 6** Variation of elevation of dam body versus time during construction





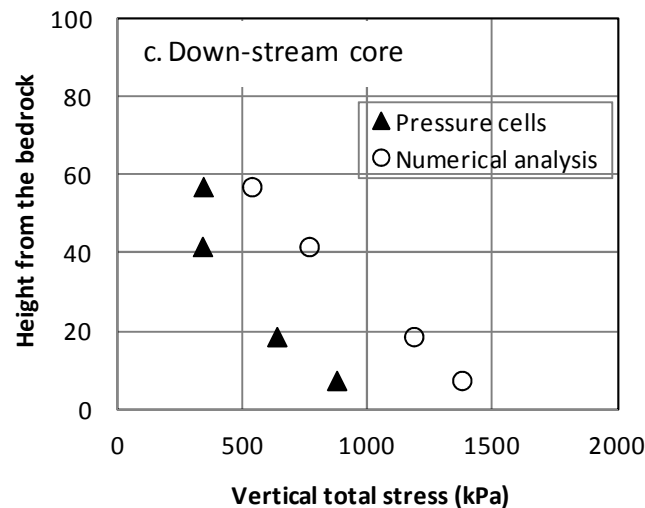


**Fig. 7** Comparison of vertical total stresses at the end of construction for a. up-stream, b. center, and c. down-stream of the core

**Table 5** Comparison of the vertical stress and arching ratio at the end of construction

| Cell No. | Location          | Distance to axis | Height of Installation from the bedrock (m) | Instruments           |       | Numerical analysis    |       |
|----------|-------------------|------------------|---|-----------------------|-------|-----------------------|-------|
|          |                   |                  |   | Vertical total stress | $A_r$ | Vertical total stress | $A_r$ |
| CPC1     | Core center       | -0.5             | 77.1  | 183                   | 0.66  | 230                   | 0.83  |
| CPC2     | Down-stream shell | -43.4            | 57  | 321                   | -     | 446                   | -     |
| CPC3     | Down-stream core  | -10.5            | 57  | 343                   | 0.54  | 537                   | 0.85  |
| CPC4     | Up-stream core    | 10.2             | 57  | 220                   | 0.34  | 521                   | 0.83  |
| CPC5     | Up-stream shell   | 45               | 57.2  | 139                   | -     | 362                   | -     |
| CPC6     | Down-stream shell | -45              | 37  | Damaged               | -     | 877                   | -     |
| CPC7     | Down-stream core  | -17              | 41.6  | 340                   | 0.39  | 766                   | 0.88  |
| CPC8     | Core center       | 0                | 41.7  | 485                   | 0.49  | 818                   | 0.83  |
| CPC9     | Up-stream core    | 18.2             | 41.6  | 450                   | 0.51  | 731                   | 0.83  |
| CPC10    | Up-stream shell   | 45               | 37  | 806                   | -     | 829                   | -     |
| CPC11    | Down-stream shell | -45              | 17.5  | Damaged               | -     | 1313                  | -     |
| CPC12    | Down-stream core  | -20              | 18.1  | 637                   | 0.48  | 1184                  | 0.90  |
| CPC13    | Core center       | 0.1              | 18.7  | Damaged               | -     | 1247                  | 0.86  |
| CPC14    | Up-stream core    | 20.3             | 18.3  | 719                   | 0.54  | 1154                  | 0.88  |
| CPC15    | Up-stream shell   | 45               | 18.1  | 870                   | -     | 1317                  | -     |
| CPC16    | Down-stream core  | -20.4            | 7.3   | 876                   | 0.57  | 1376                  | 0.89  |
| CPC17    | Core center       | 0.2              | 7.5   | 740                   | 0.44  | 1439                  | 0.86  |
| CPC18    | Up-stream core    | 19.8             | 7.3   | 748                   | 0.49  | 1352                  | 0.88  |

As demonstrated by the results, there was a significant difference between the observed and calculated vertical stresses; the vertical stresses in the pressure cells were lower than those obtained by the numerical analysis. There were some reasons as why such a behavior occurred in the core. Calibration of the instruments for load and temperature is a difficult and expensive task so that lack of calibration and destruction of instruments is assumed possible [12]. In addition, to prevent damage to the pressure cells, the soil around the cells was compacted in a lower density in comparison to other parts of the core. Therefore, the local arching in the place of instruments led to altering elasticity modulus and density around the pressure cells. Consequently, the reality of the soil stiffness in the body of the dam was more than that around the cells [3, 12]. On the other hand, the shape of a valley affects the stress distribution in an earth dam. In a U-shape valley, plane strain condition is a logical consideration and a 2D-analysis somehow explains the mechanical behavior

of the dam. On the contrary, in a V-shape valley, this assumption is far from the reality and needs a three-dimensional modeling of the earth dam. Some researchers have stated that the two-dimensional modeling of an earth dam leads to appropriate results provided that the length-to-height ratio of the earth dam is higher than 6. Otherwise, a three-dimensional modeling should be considered [18]. For Vanyar dam, this ratio was about 3.1 (286 m in length and 91 m in height). Consequently, to reach accurate results for Vanyar dam, a three-dimensional modeling was needed. In addition, the arching phenomenon between the body of the dam and the V-shape slopes of the valley can be another reason for justifying the stress differences between the instruments and the numerical analysis in Vanyar dam [18]. According to the settlement results, it can be concluded that the material properties had suitable accuracy and were not a source of error in the calculated stresses. In fact, in the finite element procedure, at first, the deformations were

calculated through solving a linear set of equations and, then, stresses were calculated from the deformation results. Table 5 shows a significant difference between the arching ratio obtained from the instrument data and those calculated by the numerical analysis. It refers to the difference in vertical stresses obtained by the pressure cells and numerical analysis. Furthermore, the arching ratio in Vanyar dam was between 0.83 and 0.90, showing that the dam was located on a safe side in terms of hydraulic fracturing at the end of construction.

#### 4.3. Pore water pressure

Pore water pressures in the core of Vanyar dam were recorded using various types of piezometers. Location of the piezometers in cross-section C is shown in Fig.1. In addition, the pore water pressures, obtained from the

numerical analysis, were compared to those recorded by the instruments at the end of construction. Table 6 and Figs. 8a, 8b, and 8c show the variation of the pore pressure for up-stream, center, and downstream of the core, respectively. The pore water pressure ratios are defined in the following equations:

$$r_u = \frac{u}{\gamma h} \quad (4)$$

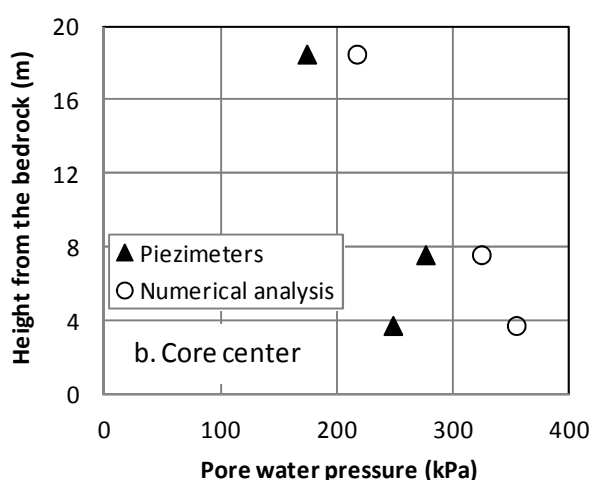
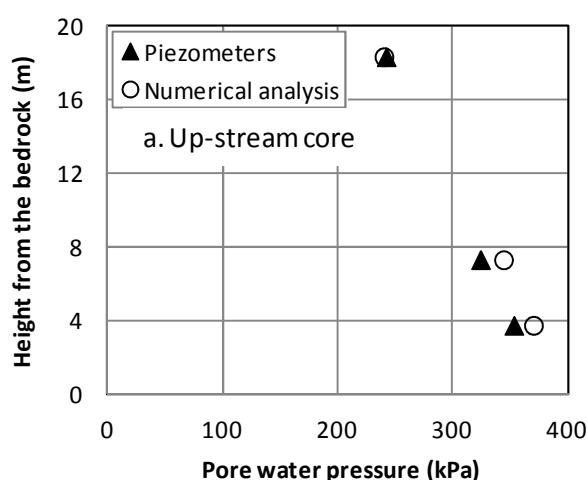
$$R_u = \frac{u}{\sigma_v} \quad (5)$$

where  $u$  is pore water pressure at the point,  $\gamma$  is unit weight,  $h$  is soil layer thickness above the point, and  $\sigma_v$  is total vertical stress at the point.

**Table 6** Comparison of the results of pore pressure ratios for vibrating and Casagrande piezometers with the results of numerical analysis at the end of construction

| Piezometer No. | Location         | Distance to axis | Installation height (m) | Pore pressure |                    | $r_u$       |                    | $R_u$       |                    |
|----------------|------------------|------------------|-------------------------|---------------|--------------------|-------------|--------------------|-------------|--------------------|
|                |                  |                  |                         | Instruments   | Numerical analysis | Instruments | Numerical analysis | Instruments | Numerical analysis |
| CVP7*          | Down-stream core | -20              | 18                      | 105           | 221                | 0.08        | 0.17               | 0.16        | 0.19               |
| CVP8           | Core center      | 0                | 18.5                    | 174           | 217                | 0.12        | 0.15               | -           | 0.17               |
| CVP9           | Up-stream core   | 20               | 18.3                    | 242           | 240                | 0.18        | 0.18               | 0.33        | 0.21               |
| CVP10          | Down-stream core | -20.6            | 7.5                     | 321           | 332                | 0.21        | 0.22               | 0.37        | 0.24               |
| CVP11          | Core center      | 0.4              | 7.6                     | 276           | 324                | 0.16        | 0.19               | 0.37        | 0.22               |
| CVP12          | Up-stream core   | 19.8             | 7.3                     | 324           | 344                | 0.21        | 0.23               | 0.43        | 0.25               |
| CSP1**         | Down-stream core | -16.2            | 3.75                    | 256           | 360                | 0.17        | 0.21               | -           | 0.25               |
| CSP2           | Core center      | -3.8             | 3.75                    | 248           | 354                | 0.14        | 0.2                | -           | 0.24               |
| CSP3           | Up-stream core   | 15.9             | 3.75                    | 353           | 370                | 0.21        | 0.22               | -           | 0.26               |

\*Vibration piezometer; \*\*Casagrande piezometer



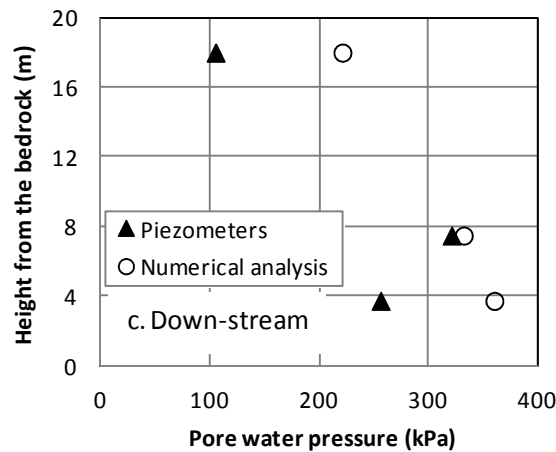


**Fig. 8** Comparing of the pore water pressures obtained from the numerical analysis and the instruments at the end of construction for a. core up-stream, b. core center, and c. core down-stream

Relative stability of  $r_u$  during and at the end of the construction showed the suitable speed of construction and, therefore, hydraulic fracturing was improbable. In addition, the low value of  $R_u$  indicated high reliability against hydraulic fracturing due to the arching phenomenon.  $R_u$  value is generally more than  $r_u$  in the core. According to Fig. 8, there were some differences between the pore pressure recorded by the instruments and that by the numerical analysis, because the saturation ratio and permeability during numerical modeling were assumed constant in the core, whereas, in reality, these two parameters alter in the height of the dam. The data recorded by the piezometers installed in the depth of the dam (Fig. 8) showed that maximum differences of pore pressure between the instruments and numerical analysis occurred at the lowest level of the dam core.

Some of those differences were due to the delay in the piezometer response and damage to the piezometers, such as tilted tubes and congestion with soil during embankment operations around the instruments. As for conducting the numerical analysis, some purposes were pursued, which included considering the isotropic traits of the dam materials, estimating numerical modeling to simulate the seepage condition at the end of the construction, and approximating  $\theta_w$  function without doing any laboratory test that would affect the numerical results. In addition, Table 6 shows that the observed and calculated  $r_u$  were in good agreement at the end of the construction. Difference between the observed and calculated  $R_u$  was due to the difference between the observed and calculated vertical stresses. In addition, maximum calculated  $R_u$  reached 0.26 in the core, while maximum  $R_u$  recorded by the instruments was about 0.43. According to the technical report of Vanyar dam [15], the predicted  $R_u$  in the design stage was 0.5, which provided the dam safety in terms of strength against hydraulic fracturing.

## 5. Conclusion

In this research, the results of monitoring and numerical analysis of Vanyar dam were evaluated in its largest cross-section C by focusing on the settlements,

total vertical stresses, and pore water pressures. The numerical analysis showed that the mechanical characteristics and material properties extracted from laboratory tests were rather accurate. The results gained from this study are as follows:

1. According to the numerical analysis, the settlement results were consistent with the data recorded by the instruments in terms of both quality and quantity, showing that maximum settlement was 1 m on the dam axis and 46 m above the bedrock nearly in the middle of the dam height ( $\frac{z}{h} = 0.51$ ). In addition, maximum settlement of 0.83 m was recorded on the dam axis, 40 m above the bedrock ( $\frac{z}{h} = 0.44$ ). The aforementioned maximum settlements showed that both values were at the rate of about 1% of the height of the dam. Difference of the settlements between the instrument data and the numerical analysis was due to the initial delay in supplying and installing the settlement tubes. Therefore, there were no recordings by the instruments during the construction within this limited time and the observed differences were probably due to this problem.

2. Total vertical stresses, extracted from the numerical analysis, proved to be in a tolerable trend with the data recorded at the pressure cells; but, there was a significant difference from quantity. Inconsistency between the stresses obtained from the numerical analysis and pressure cells was mostly due to the local arching phenomena in the installation place of the pressure cells, which was due to inadequate compaction around these instruments that caused creating a low-stress zone. In addition, for Vanyar dam, length-to-height ratio was about 3.1 (286 m in length and 91 m in height). Consequently, to obtain accurate results, a three-dimensional model should be assumed for the numerical analysis. The arching ratios were calculated for the largest cross-section of Vanyar dam. There was a significant difference between the calculated arching ratios obtained from the numerical analysis and the data recorded by the instruments, which was due to the distinction between the vertical stresses recorded by the pressure cells and those obtained from the numerical analysis. The results demonstrated that the arching ratio in Vanyar dam was 0.83 to 0.90, which

placed the dam on the safe side in terms of hydraulic fracturing at the end of construction.

3. The pore pressure extracted from the numerical analysis and the one from the piezometers were in good agreement at the end of the construction. Difference between the observed and calculated  $R_u$  was due to the difference between the observed and calculated vertical stresses. Furthermore, maximum calculated  $R_u$  reached 0.26, while maximum  $R_u$  recorded by the instruments was about 0.43 in the core of the dam. The predicted  $R_u$  at the design stage was 0.5, which provided the dam safety in terms of strength against hydraulic fracturing.

Finally, it is worth mentioning that the behavior of this dam in its largest cross-section C was reasonable in terms of settlement, stresses, and pore water pressure. Owing to the dam geometry and shape of the valley, it is recommended to use three-dimensional finite element modeling for gaining better understanding about the behavior of Vanyar dam.

## References

- [1] Yu Y, Zhang B, Yuan H. An intelligent displacement back-analysis method for earth-rockfill dams, *Computers and Geotechnics*, 2007, Vol. 34, pp. 423-434.
- [2] Clough RW, Woodward RJ. Analysis of embankment stresses and deformations, *Journal of the Soil Mechanics and Foundations Division*, 1967, No. SM4, Vol. 93, pp. 529-549.
- [3] Naylor D, Maranha J, Neves EMD, Pinto AV. A back-analysis of Beliche Dam, *Geotechnique*, 1997, Vol. 47, pp. 221-233.
- [4] Hunter G, Fell R. The Deformation behaviour of embankment dams, University of New South Wales, School of Civil and Environmental Engineering UNICIV Report No. R-416, 2003.
- [5] Gikas V, Sakellariou M. Settlement analysis of the Mornos earth dam (Greece): Evidence from numerical modeling and geodetic monitoring, *Engineering Structures*, 2008, Vol. 30, pp. 3074-3081.
- [6] Zhou W, Hua J, Chang X, Zhou C. Settlement analysis of the Shuibuya concrete-face rockfill dam, *Computers and Geotechnics*, 2011, Vol. 38, pp. 269-280.
- [7] Roosta RM, Alizadeh A. Simulation of collapse settlement in rockfill material due to saturation, *International Journal of Civil Engineering*, 2012, Vol. 10, pp. 93-99.
- [8] Dong W, Hu L, Yu YZ, Lv H. Comparison between Duncan and Chang's EB model and the generalized plasticity model in the analysis of a high earth-rockfill dam, *Journal of Applied Mathematics*, 2013, Vol. 2013, pp. 1-12.
- [9] Ghanbari A, Shams Rad S. Development of an empirical criterion for predicting the hydraulic fracturing in the core of earth dams, *Acta Geotechnica*, 2013, pp. 1-12.
- [10] Geo-studio for finite element analysis, in *Geo-Studio User's Guide*, ed: <http://www.geo-slope.com>, 2004.
- [11] Duncan JM, Chang CY. Nonlinear analysis of stress and strain in soils, *Journal of the Soil Mechanics and Foundations Division*, 1970, Vol. 96, pp. 1629-1653.
- [12] Dunnicliff J, Green G. *Geotechnical Instrumentation for Monitoring Field Performance*, ed: A Wiley Inter-science Publication, 1988.
- [13] Jaky J. The coefficient of earth pressure at rest, *Journal of the Society of Hungarian Architects and Engineers*, 1944, Vol. 78, pp. 355-358.
- [14] Henkel D. The shear strength of saturated remolded clays, in *Proceedings of the ASCE Research Conference on Shear Strength of Cohesive Soil*, Boulder, Colorado, USA, 1960, pp. 533-554.
- [15] Technical reports of Vanyar dam, Ghods-Niroo consultant engineers Co, Tehran, 2011.
- [16] Terzaghi K. Stress distribution in dry and in saturated sand above a yielding trap-door, in *Proceeding of First International Conference on Soil Mechanics and Foundation Engineering*, Cambridge, Massachusetts, 1936, pp. 307-311.
- [17] Terzaghi K. *Theoretical Soil Mechanics*, New York, John Wiley and Sons, 1943.
- [18] Lefebvre G, Duncan J, Wilson E. Three-dimensional finite element analysis of dams, *Journal of the Soil Mechanics and Foundations Division*, 1973, No. SM7, Vol. 99, pp. 495-507.